Journal of Volcanology and Geothermal Research 371 (2019) 206–219

Contents lists available at ScienceDirect

Journal of Volcanology and Geothermal Research

journal homepage: www.elsevier.com/locate/jvolgeores

Eruption frequency patterns through time for the current (1999–2018) activity cycle at Volcán de Fuego derived from remote sensing data: Evidence for an accelerating cycle of explosive paroxysms and potential implications of eruptive activity

Ailsa K. Naismith [a,*], I. Matthew Watson [a], Rüdiger Escobar-Wolf [b], Gustavo Chigna [c], Helen Thomas [a], Diego Coppola [d], Carla Chun [c]

[a] School of Earth Sciences, Wills Memorial Building, University of Bristol, Queens Road, Bristol BS8 1RJ, United Kingdom
[b] Department of Geological and Mining Engineering and Sciences, Michigan Technological University (MTU), 630 Dow Environmental Sciences, 1400 Townsend Drive, Houghton, MI 49931, United States of America
[c] Instituto Nacional de Sismología, Vulcanología, Meteorología e Hidrología (INSIVUMEH), Edificio Central, 7a. Avenida 14-57 Zona 13, Guatemala, Guatemala
[d] Dipartimento di Scienze della Terra, Università degli studi di Torino, Via Valperga Caluso 35, 10125 Torino, Italy

ARTICLE INFO

Article history:
Received 10 August 2018
Received in revised form 7 December 2018
Accepted 1 January 2019
Available online 6 January 2019

Keywords:
Volcán de Fuego
Paroxysm
MIROVA
Radiative power

ABSTRACT

Volcán de Fuego is a stratovolcano in Guatemala that has produced over 50 VEI ≥ 2 eruptions since 1524. After two decades of quiescence, in 1999 Fuego entered a new period of eruptive activity that continues until the present day, characterized by persistent Strombolian activity interspersed with occasional "paroxysmal" eruptions of greater magnitude, the most recent of which occurred in 2018. The land surrounding Fuego accommodates tens of thousands of people, so greater understanding of its eruptive behaviour has important implications for hazard assessment. Nevertheless, there is relatively little literature that studies recent (since 1999) activity of Fuego in detail.

Using time-series analysis of remote sensing thermal data during the period 2000–2018 combined with recent bulletin reports, we present evidence for a new eruptive regime beginning in 2015. We find that this regime is defined by a greater frequency of paroxysmal eruptions than in previous years and is characterized by the following sequence of events: (i) effusion of lava flows and increase in summit explosive activity, followed by (ii) an intense eruptive phase lasting 24–48 h, producing a sustained eruptive column, continuous explosions, and occasional pyroclastic flows, followed by (iii) decrease in explosive activity. We discuss various models that explain this increase in paroxysmal frequency, and consider its implications for hazard assessment at Fuego. We advocate the pairing of remote sensing data with monitoring reports for understanding long-term changes in behaviour of poorly-instrumented volcanoes. The results that we present here provide a standard for informed assessment of future episodes of unrest and paroxysmal eruptions of Fuego.

1. Introduction

Volcán de Fuego (3763 m asl; 14.47°N, 90.88°W), a prominent stratovolcano in southern Guatemala, produced a large eruption on 3rd June 2018 that generated pyroclastic flows and caused extensive damage and death in nearby communities. Despite being highly active, there is a paucity of recent literature on the volcano. To provide context for this and other recent eruptions, we present an overview of the eruptive history of Fuego gathered from available academic literature. We also present new evidence, derived from long-term seismic and thermal databases, that points to the onset of a new cyclical eruptive regime.

"Volcán de Fuego" translates from Spanish as "Volcano of Fire". One of the first documented eruptions of Fuego exists in the letters of the *conquistador* Pedro de Alvarado, who recorded its activity in 1524 (Kurtz, 1913). Fuego was also known for its ferocity to the Maya people, who christened it "Chiq'aq", meaning "Fireplace" in the indigenous Quiché language (Tedlock, 1985). With over 50 Volcanic Explosivity Index (VEI) ≥ 2 eruptions recorded since 1524, Fuego is one of the most active volcanoes in Central America (Global Volcanism Program, 2018), with a history of producing both violent Strombolian (Berlo et al., 2012; Waite et al., 2013) and sub-Plinian eruptions (Rose et al., 2008; Escobar-Wolf, 2013). During periods of activity, Fuego's

* Corresponding author.
E-mail addresses: ailsa.naismith@bristol.ac.uk (A.K. Naismith), Matt.Watson@bristol.ac.uk (I. Matthew Watson), rpescoba@mtu.edu (R. Escobar-Wolf), diego.coppola@unito.it (D. Coppola).

https://doi.org/10.1016/j.jvolgeores.2019.01.001
0377-0273/

behaviour consists of a persistent background of low-intensity Strombolian eruptions and ash-rich explosions (Patrick et al., 2007), which are interspersed with discrete events of larger energy and violence, referred to in this paper as "paroxysms" (see Section 2 for full definition) (Martin and Rose, 1981; INSIVUMEH, 2012a, 2012b). Fuego's periods of activity occur between periods of repose lasting up to several decades (Martin and Rose, 1981). A series of sub-Plinian eruptions in 1974 produced 0.2 km^3 of basaltic tephra that spread 200 km W (Rose et al., 2008). This eruptive episode remains the largest since 1932. Since 1999, Fuego has been in a new period of eruptive activity (Lyons et al., 2010). This period, like those before it, is dominated by persistent Strombolian activity producing lava fountaining and explosions and punctuated by occasional paroxysmal eruptions of greater energy and violence producing lava flows and (less frequently) pyroclastic flows (Escobar-Wolf, 2013; Rader et al., 2015).

In this paper, we use volcano radiative power (VRP) values from the Middle InfraRed Observation of Volcanic Activity (MIROVA) database (Coppola et al., 2016) to study recent eruptive activity at Volcán de Fuego. The method we use is based on the approach by Coppola et al. (2012), analysing thermal output associated with volcanic activity at Stromboli between 2000 and 2011. In addition, our analysis is focussed on correlating trends observed in the MIROVA Fuego data with records of eruptive activity from the *Instituto Nacional de Sismología, Vulcanología, Meteorología e Hidrología* (INSIVUMEH), Guatemala's national scientific monitoring agency, and other datasets including Real-Time Seismic Amplitude Measurement (RSAM) values (INSIVUMEH, 2018) and Washington Volcanic Ash Advisory (VAA) reports (National Oceanic and Atmospheric Administration (NOAA), 2019).

Paroxysmal eruptions at Fuego have been documented in previous literature, which has discussed various models that may trigger these events (e.g. Lyons et al., 2010). However, the majority of such literature appeared prior to the eruptive activity discussed in this paper. Therefore, we review the models for triggering paroxysm at Fuego and consider factors that may cause the observed increase in paroxysmal frequency since 2015. Furthermore, we examine the impacts of Fuego's eruptive hazards on exposed populations and infrastructures through study of specific paroxysmal eruptions occurring since 2015, including the eruption of 3rd June 2018.

2. Eruptive history of Volcán de Fuego

Forecasting the effects of future eruptions is inevitably informed by an understanding of past eruptions. This understanding includes a brief introduction to Fuego's tectonic setting, which has implications for the characteristics of volcanism observed. The majority of academic literature on Fuego's eruptive behaviour can be classified into one of three categories: prehistoric (before records began in 1524), historic (16th–20th century), or recent (1999–present). A full summary of notable eruptive events at Fuego during the historic and recent categories can be found in supplementary material (Appendix A).

Fuego is located close to the triple junction of the North American, Cocos, and Caribbean tectonic plates (Fig. 1 inset). The complex interplay of compressive and translational forces between these plates controls the behaviour of the Central American volcanic arc (Álvarez-Gómez et al., 2008; Authemayou et al., 2011), which is divided into seven segments of volcanic lineaments, of which Fuego occupies the furthest north (Stoiber and Carr, 1973; Burkart and Self, 1985). Fuego is part of the Fuego-Acatenango massif, a volcanic complex consisting of five known eruptive centres younging towards the south (Fig. 1) (Vallance et al., 2001). The earliest evidence of volcanic activity at this complex is a lava flow dated to 234,000 ± 31,000 years; however, most of the complex was constructed after the Los Chocoyos ash eruption from nearby Lake Atitlan, 84,000 years ago (VanKirk and Bassett-VanKirk, 1996; Vallance et al., 2001). At least two edifice collapse events have occurred since. The most recent, the collapse of La Meseta's eastern flank between 30,000 and 8500 years ago, delivered over 9 km^3 of material to slopes to the south (Vallance et al., 1995), extinguishing activity at La Meseta and allowing for the subsequent development of volcanic activity that would eventually build Fuego (Martin and Rose, 1981; Vallance et al., 2001).

Fuego is the currently most active volcanic centre of the Fuego-Acatenango massif and has an upper age limit of 30,000 years (Vallance et al., 2001). A minimum age of 8500 years for Fuego has been calculated by extrapolating from a calculated effusion time for a sequence of lavas on Meseta's flank (Chesner and Rose, 1984). An alternative minimum age of 13,000 years has been calculated by extrapolating from an estimated average eruption rate of 1.7×10^9 m^3 across the last 450 years (Martin and Rose, 1981).

Extremely little stratigraphic data exist for prehistoric eruptive activity at Fuego. This is in part because Fuego does not typically produce deposits that are sufficiently unique to be easily dated and thus constrain stratigraphic evolution. Some evidence for previous eruptions producing pyroclastic flows exists in the form of flow deposits that have been estimated by radiocarbon dating at 5370 ± 50, 3560 ± 70, 2170 ± 30, 1375 ± 45, 1050 ± 70, and 980 ± 50 years old (Vallance et al., 2001; Escobar-Wolf, 2013). Analysis of lava samples obtained from exposures in two of Fuego's drainage ravines (*barrancas*), Barrancas Honda and Trinidad, reveals that prehistoric activity at Fuego has produced basalts, basaltic andesites, and andesitic lavas, with an evolution with time towards more mafic eruptive products. Prehistoric eruptive products were derived from fractional crystallization of plagioclase, olivine, augite, and magnesite from a basaltic melt rich in Al_2O_3 (Chesner and Rose, 1984).

The volume of information on Volcán de Fuego's eruptive activity improved greatly with the beginning of modern record-keeping that arrived with the Spanish in 1524. Records of a volcano's historic eruptive activity are rarely fully comprehensive, and those of Fuego are no exception. However, the greater the magnitude the eruption, the more certain the information (Escobar-Wolf, 2013). A summary of Fuego's eruptive activity between 1524 and 1999 illustrates that Fuego's occasional sub-Plinian and persistent Strombolian behaviours are interspersed with extended periods of repose lasting for years or even decades (Fig. 2). The majority of eruptions of Fuego are contained within short intervals between repose: four periods of 20–70 years account for 75% of activity since 1524 (Hutchison et al., 2016); these include at least five VEI 4 eruptions that have occurred between 1524 and the present day: in the years 1581–2, 1717, 1880, 1932 and 1974 (Escobar-Wolf, 2013; Hutchison et al., 2016; VOGRIPA, 2018). Because physical volcanology is a young science, there is no single measure existing for all these eruptions by which to closely compare their relative magnitudes. However, several details suggest that some of the earlier eruptions were at least equivalent in magnitude to those of 1974. An account of the eruption in January 1582, for instance, states "in the twenty four hours that the fury lasted, one couldn't see anything from the volcano but rivers of fire and very large rocks made embers, which came out of the volcanoes mouth and came down with enormous fury and impetus" (de Ciudad-Real, 1873). This account of 24 h of paroxysmal activity, including violent ejection of ballistics and possible pyroclastic flows, is comparable to some of the larger paroxysmal eruptions observed in Fuego's more recent eruptive history.

Records of the 1717 eruption are well-preserved and give a decent chronology of the activity. The main phase of the eruption lasted between 27th and 29th August when locals heard rumbles and explosions from Fuego's summit. People reported glowing clouds and fiery phenomena, assumed to be pyroclastic flows (Hutchison et al., 2016). On 29th September several earthquakes followed the eruption, in turn triggering mudflows apparently originating from nearby Volcán de Agua (Hutchison et al., 2016). However, reports of damages to the communities of Mixtan and Masagua on the Río Guacalate, beyond the confluences of drainages from Fuego and Agua volcanoes, suggest that at least some of these mudflows originated from Fuego. An anonymous account of the eruption of 29th June 1880 states that people in

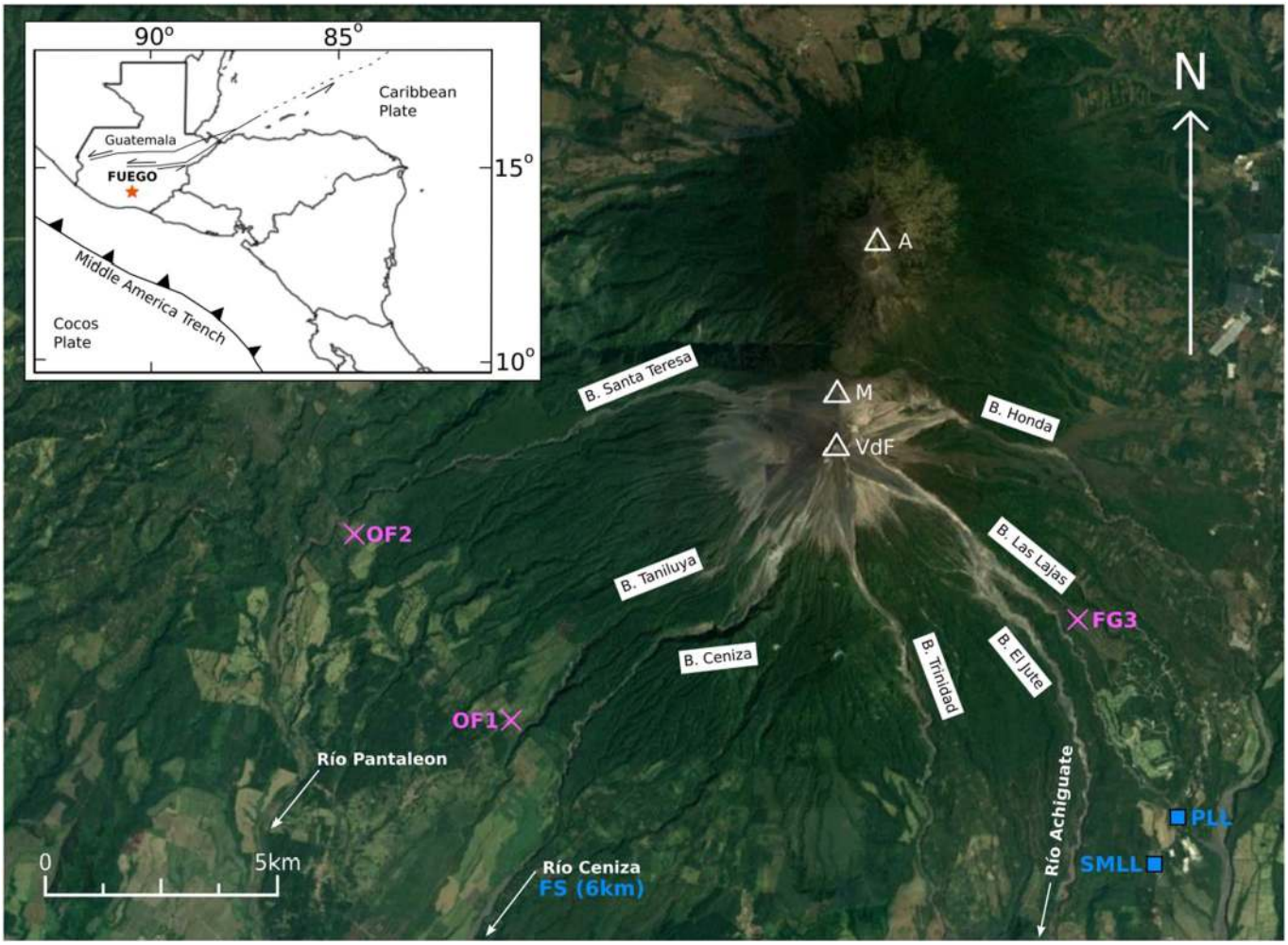

Fig. 1. Map of Volcán de Fuego including its seven *barrancas* (drainage ravines) and major *ríos* (rivers), with (inset) location of Fuego within Guatemala. Barrancas of Fuego control movement of lava flows, pyroclastic flows, and lahars. Principal eruptive centres of the Fuego-Acatenango massif are (north to south) Volcán Acatenango (indicated as A), La Meseta (M) and Volcán de Fuego (VdF). INSIVUMEH's two Fuego observatories, OVFGO1 and OVFGO2, are located respectively in the villages of Panimaché Uno and Sangre de Cristo and are indicated by pink crosses. They are labelled as "OF1" and "OF2". INSIVUMEH's short-wave seismometer, that provided RSAM data in Section 4, is labelled as "FG3" and indicated by a pink cross. Blue labels indicate the community of San Miguel Los Lotes (SMLL), the Las Lajas bridge (PLL), and the Scout encampment (FS), located approximately 6 km south of map's southern extent down Barranca Ceniza.
Map data: Google Earth V 7.1.8.3036 (2018).

Mazatenango and Retalhuleu had to write by artificial light, because of "dense darkness … caused by a thick and continuous ash rain, thrown without a doubt by the volcano from whose eruption we have been talking about" (Feldman, 1993). The cities of Mazatenango and Retalhuleu are 67.5 km and 85.9 km respectively from Fuego, showing the extensive tephra dispersal of the 1880 eruption.

An important account of the January 1932 eruption comes from Degger (1932). Strong earthquakes were felt on the morning of 21st January as far as Livingstone (on the Caribbean coast of Guatemala) and in neighbouring Honduras and El Salvador. The original eruption column was estimated at 17,000 ft asl (~5200 m). The episode generated an extremely large and long-ranging tephra blanket: fine ash fall was observed in many places throughout Guatemala, and close to Fuego the fall of clasts as large as pebbles and cobbles was reported (Degger, 1932). The morphology of the summit crater was changed by the eruption, and its diameter greatly increased (Degger, 1932).

Fuego was particularly active in the 1970s. Eruptions in September 1971 and February 1973 were comparable in size to each of the individual eruptions composing the sub-Plinian eruptive episode of 1974 (Bonis and Salazar, 1973; Martin and Rose, 1981). The eruption of 14th September 1971 was particularly impressive: a report from the Instituto Geográfico Nacional (IGN) states, "All observers agree this was the most spectacular eruption in memory (at least 70 years)" (GVP, 2018). The 1971 eruption began suddenly and lasted 12 h, producing an eruptive column of 10,000 m asl and extensive pyroclastic flows (Bonis and Salazar, 1973). Flows travelled E down Barranca Honda, but the direction of ash dispersal was W towards the departments of Acatenango and Yepocapa. Approximately one fifth of roofs in the town of San Pedro Yepocapa, 8 km W of Fuego, collapsed under the weight of ash fallen, estimated at 30 cm depth (Bonis and Salazar, 1973; GVP, 2018). The eruption of 1973 was longer but less powerful than that of 1971, although the flows produced in 1973 were both longer and more voluminous than in 1971 (Bonis and Salazar, 1973). The majority of activity occurred between 22nd February and 3rd March 1973, producing pyroclastic flows on Fuego's SW, W and E flanks, and ash that was dispersed to a distance of 70 km (Bonis and Salazar, 1973; GVP, 2018).

The 1971 and 1973 eruptions likely awakened both local and academic interest in Fuego's activity (Bonis and Salazar, 1973). They may explain the wealth of academic literature on the sub-Plinian eruptive episode that occurred in October 1974, which is one of the most well-documented volcanic eruptions of Central America (Roggensack, 2001). Between 10th and 23rd October 1974, Fuego produced four powerful eruptions that generated extensive tephra and multiple pyroclastic

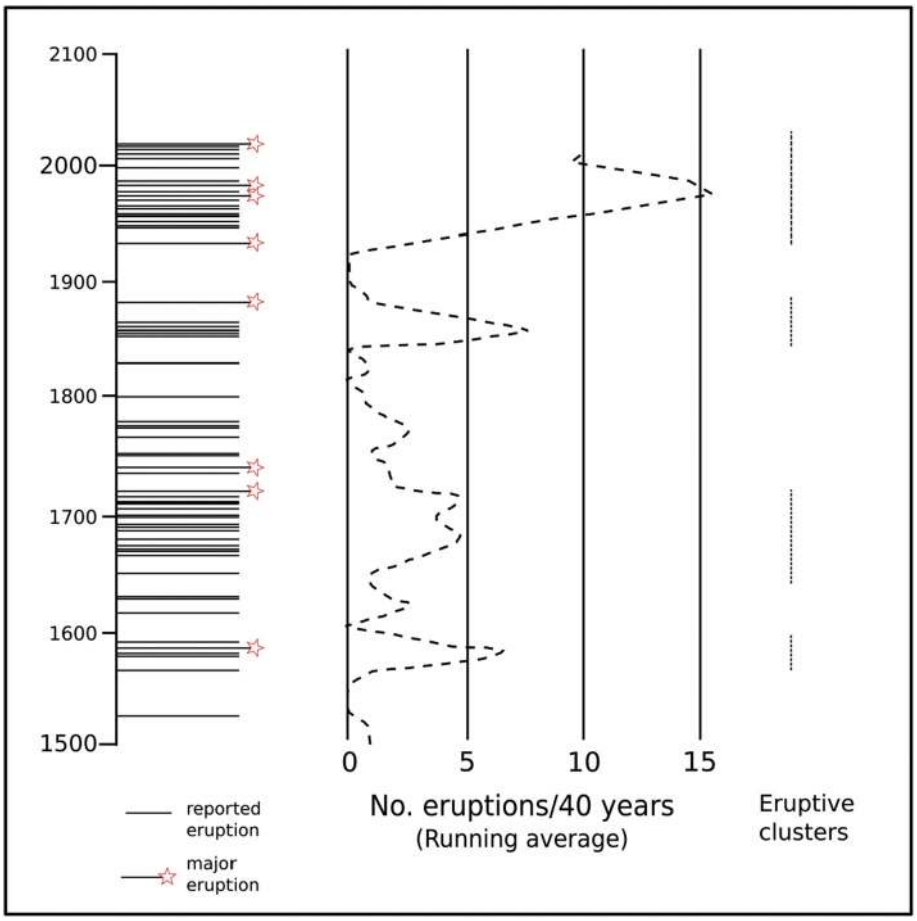

Fig. 2. Historic activity of Fuego since 1524. Modified from Rose et al. (1978) via Vallance et al. (2001) and GVP (2018). Four eruptive clusters of 20–70 years have defined the eruptive history of Fuego since 1524. Significant eruptions in 1581–2, 1717, 1737, 1880, 1932, 1971, 1974, 1999 and 2018 have been highlighted by red stars.

flows (Davies et al., 1978; Rose et al., 2008). Tephra from Fuego again collapsed roofs in San Pedro Yepocapa and spread to the capital, [Ciudad de] Guatemala, located 40 km E of Fuego and then with a population of over a million (Vallance et al., 2001). The most violent of these four eruptions began at 21:45 on 17th October, with an eruption that sustained a plume reaching >7 km above Fuego's summit (>11 km asl) (Rose et al., 1978). No lava flows were produced in the October eruptive episode (Davies et al., 1978). Instead, the fortnight of activity produced an extraordinary volume of tephra and pyroclastic flows that descended several of Fuego's barrancas, reaching a maximum of 8 km from the volcano's summit (Escobar-Wolf, 2013). Estimates of eruptive volume produced during the fortnight range from 0.2 km^3 of tephra (0.1 km^3 dense rock equivalent, DRE) (Rose et al., 1978), to 0.6 km^3 of tephra and glowing avalanche material (Davies et al., 1978).

The sub-Plinian eruption in 1974 was followed by several small eruptions of Fuego between 1975 and 1978 (Rose et al., 1978). These eruptions were succeeded by two decades of quiescence (1979–1999), interrupted only briefly by small Strombolian eruptions in 1987 and 1988 (Andres et al., 1993). The extended quiescence accounts for the relative dearth of literature published on Volcán de Fuego during this period.

Volcán de Fuego erupted again on 21st May 1999 with a VEI 2 eruption that produced pyroclastic flows and tephra fall (Lyons and Waite, 2011). Fuego's eruptive activity since 1999 has been dominated by open-vent conditions producing Strombolian activity, summit explosions, persistent degassing, and lava flows (Fig. 3). However, between 1999 and 2012, with a hiatus between the years 2008 and 2011, Fuego also consistently produced several eruptive events each year that were of greater energy and duration than typical Strombolian behaviour (INSIVUMEH, 2012a, 2012b). These events are referred to by INSIVUMEH as "paroxysms" or "paroxysmal eruptions", and we will use these terms throughout this paper also. Our definition of a "paroxysm" or "paroxysmal eruption" at Volcán de Fuego is based on a group of characteristics shared by these events that have occurred since 1999 and been classified in previous literature (Lyons et al., 2010). In agreement with other authors, we define a paroxysmal eruption at Fuego as an above-background eruptive event consisting of a three-stage process: (i) a waxing phase, involving effusion of lava flows and an increase in frequency and energy of intermittent gas chugging and Strombolian explosions at summit, persisting for 24–48 h; preceding (ii) a climax in explosive activity, the "paroxysm" itself, involving maintained effusion of lava flows and continuous explosions sustaining an eruptive plume of fine ash and gas, with intermittent production of pyroclastic flows; succeeded by (iii) a subsequent waning of activity (Lyons et al., 2010). A good example of a paroxysmal eruption at Fuego is the description of the 13th September 2012 eruption found in the preliminary report released by INSIVUMEH (2012a, 2012b, *Reporte Preliminar*).

Some of Fuego's paroxysms have caused significant disruption to surrounding communities. For instance, between January and August 2003, several communities were evacuated due to eruptive activity of Fuego, activity that included a paroxysmal eruption in January (Webley et al., 2008). Several paroxysmal events between 1999 and 2012 have been deemed significant by INSIVUMEH due to the greater volume of fine ash and pyroclastic flows they generated: 21st May 1999; 9th February 2002; 8th January 2003; 29th June 2003 (which

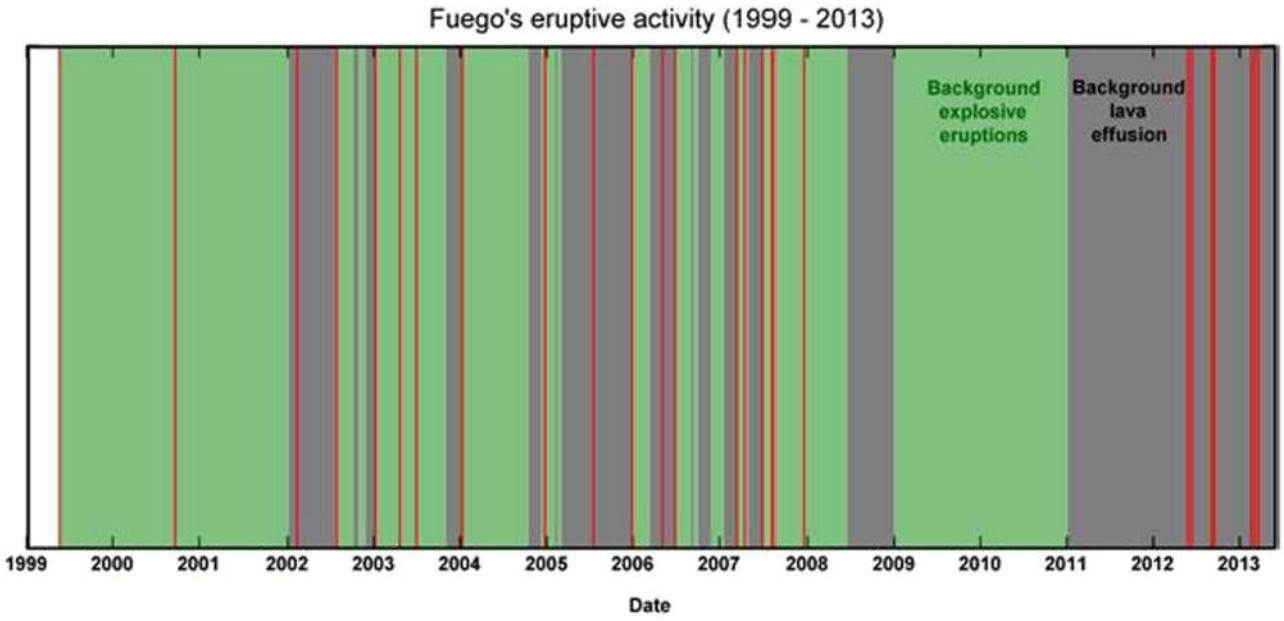

Fig. 3. Time-series illustrating activity of Fuego between 1999 and 2013, with colour bars representing different eruption styles. Activity in early 2000s and 2009–2011 was dominated by background explosive eruptions (green), while background effusive activity dominated between 2005–2007 and 2011–2013 (grey). Episodes of significantly above-background explosive activity (paroxysms) illustrated in red.
From GVP (2018), originally created by Rüdiger Escobar-Wolf.

completely filled Barranca Santa Teresa with pyroclastic flow deposits); 16th–18th July 2005; 5th–8th May 2006; 7th–9th August 2007; 15th December 2007; 13th September 2012; and 3rd June 2018 (INSIVUMEH, 2012a, 2012b). [For a complete list of notable (VEI ≥ 2) eruptive events at Fuego between 1524 and 2018, please refer to Appendix A.] Consistent monitoring between 2005 and 2007 revealed patterns in eruptive behaviour that tracked well with radiant heat output from MODIS and seismic RSAM values (Lyons et al., 2010). During these three years Volcán de Fuego displayed a cyclical pattern of behaviour consisting of three stages: (i) passive lava effusion and minor Strombolian explosions; (ii) paroxysmal eruptions involving a sustained eruption column and rapid lava effusion; (iii) passive degassing without lava effusion (Lyons et al., 2007, 2010). Multi-instrumental investigation of Fuego's activity between 2008 and 2009 revealed the presence of two summit crater vents, each associated with distinct styles of explosive activity. The primary central summit vent produced impulsive, powerful, ash- and bomb-rich explosions interspersed with periods of ash-free gas puffing, while a secondary vent 100 m W of the summit produced long-duration, emergent, ash-rich explosions (Nadeau et al., 2011; Waite et al., 2013). Throughout this observation period, a large variety of explosion intensities were observed. However, the largest explosions were all associated with very long period (VLP) seismic activity and showed evidence for pressurization of the upper conduit under a crystallized plug prior to explosive release (Lyons and Waite, 2011; Waite et al., 2013). More recently, detailed analysis of VLP signals has provided a means to distinguish eruptive styles at Fuego (Waite et al., 2013).

One of Fuego's largest eruptions in the period 1999–present occurred on 13th September 2012 (BBC, 2012). 48 h before eruption, an increase in long-period (LP) events was recorded, along with the appearance of a large-amplitude volcanic tremor. During this time, activity produced a 300 m lava flow on Fuego's southern flanks. Due to the increase in activity, a special bulletin was issued to Guatemala's national emergency response and disaster risk reduction agency, CONRED (*Coordinadora Nacional para la Reducción de Desastres*) (INSIVUMEH, 2012a, 2012b, *Reporte preliminar*). The eruption began at 04:00 local time on 13th September and by 07:15 an eruption column had risen 2000 m above the summit crater, causing CONRED to issue first a yellow alert ("prepare to act") and subsequently an amber alert ("evacuate if necessary").[1] Pyroclastic flows descended the southern flanks at 09:12 and CONRED escalated the alert level to the highest, red, status ("evacuate immediately") (INSIVUMEH, 2012a, 2012b, *Reporte preliminar*).

More recently, a large paroxysmal eruption of Fuego occurred on 3rd June 2018. The eruption began at 06:00 local time with powerful incandescent fountaining and a tall eruptive column. During the morning hours, pyroclastic flows descended the W flanks of Fuego. The eruption in its initial progress appeared to be a "typical" paroxysm (Pardini et al., 2019 (under review)). However, beginning at 12:00, the intensity of the paroxysm increased, and the direction of tephra dispersal and pyroclastic flow descent shifted towards the SE. Between 14:00 and 16:00, a series of pyroclastic flows descended Barranca Las Lajas, destroying a bridge and a community and causing the deaths of several hundred people (CONRED, 2018). This eruption remains the greatest in terms of human impact within Fuego's extended history.

3. Methods

3.1. Volcanic Radiative Power from MODIS-MIROVA

Thermal activity of Volcán de Fuego has been obtained by using MIROVA, an automatic volcanic-hotspot detection system based on the analysis of MODIS infrared data (Coppola et al., 2016). MODIS (MODerate resolution Imaging Spectroradiometer) is a multispectral spectroradiometer carried on board of Terra and Aqua NASA's satellites (launched on polar sun-synchronous orbit on March 2000 and May 2002, respectively). Each MODIS sensor scans the globe surface twice a day (one at night and one during the day), and collects radiance data on 36 spectral bands spanning from 0.4 to 14.4 μm. By using Middle Infrared (MIR) data acquired by MODIS, MIROVA completes automatic

[1] In the case of volcanic eruptions, CONRED has a four-colour alert system defined as follows; green ("Vigilance"): continue with normal activity; yellow ("Prevention"): prepare to act and follow authorities' instructions; amber ("Danger"): keep alert, prepare to evacuate if necessary in case of any sign of danger; red ("Emergency"): evacuate danger zones, remain in provisional shelters; follow authorities' instructions. Retrieved from: https://conred.gob.gt/site/Definicion-de-Alertas (last accessed 29/11/2018).

detection and location of high-temperature thermal anomalies and provides a quantification of the Volcanic Radiative Power (VRP) within 1 to 4 h of each satellite overpass (www.mirovaweb.it). Original MODIS Level 1B granules are resampled into an equally-spaced 1 km grid (Universal Transverse Mercator System - UTM) and cropped within a 50 × 50 km mask centred over the target volcano summit. Hotspot detection is performed by calculating spectral indices and applying spatial principles that allow identification of pixels that have middle infrared spectral radiance (L_{MIR}) that is 'anomalously high' with respect to their surroundings (see Coppola et al., 2016 for details).

The Wooster et al. (2003) formulation is then used to retrieve the VRP (W) from MODIS data starting from hot spot pixels detected by MIROVA:

$$VRP = 1.89 \times 107 \times (L_{MIR} - L_{MIRbk})$$

where L_{MIR} and L_{MIRbk} are the MIR radiances characterizing each single hot spot pixel and the background. The formula allows estimations of VRP (±30%) from hot surfaces having temperatures ranging from 600 to 1500 K. Between March 2000 and July 2018 MODIS acquired 11,639 night-time images over Volcán de Fuego. Of these, 4132 (~35%) overpasses triggered the MIROVA algorithm suggesting a continuous thermal emission throughout the whole analysed period.

3.2. Statistical determination of new eruptive regime

Following the methods of Coppola et al. (2012), a rank-ordered statistical plot of all MIROVA night-time values between January 2000 and June 2018 (n = 4412) compares the populations for Fuego between 2000–2014 and 2015–2018 (Fig. 4a). A subset of data with VRP <1 MW is related to overpasses during cloudy conditions or under extreme viewing geometries, either of which impede detection of a clear thermal anomaly. A small true thermal anomaly occurring within this subset would be impossible to distinguish from noise; therefore, we have excluded values <1 MW (illustrated by dashed line in Fig. 4a).

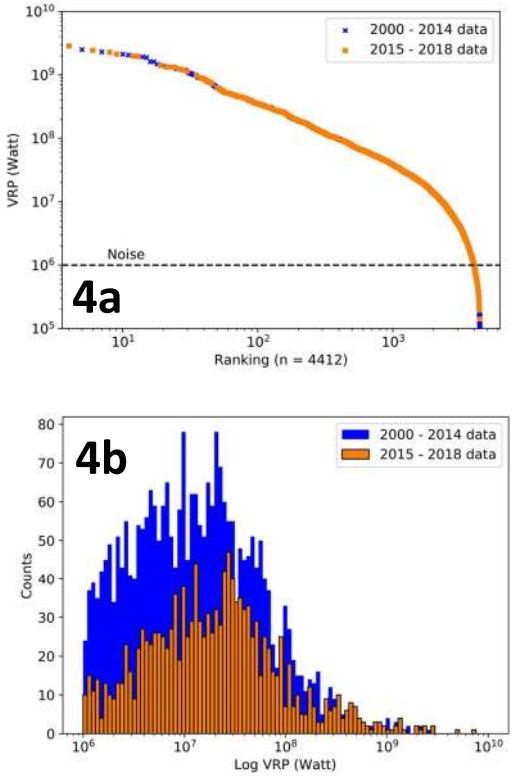

Fig. 4. a (above): rank-order plot for night-time MIROVA values of Fuego between January 2000 and June 2018 (n = 4412). b (below): histogram of two population groups (2000–2014 in blue, 2015–2018 in orange). Greater number of large VRP values in 2015–2018 dataset illustrated by skew of data towards the right of the plot.

In agreement with Coppola et al. (2012), a set of values approximating a linear trend would constitute a group of events with similar characteristics; thus, two distinct linear trends in the Stromboli MIROVA dataset illustrate a shift between Strombolian and effusive eruptive regimes. In the Fuego dataset, by contrast, a gradual shift in linear trend occurs between 1×10^6 and 3×10^7 MW of VRP. There is no clear distinction between the datasets of 2000–2014 and 2015–2018 (Fig. 4a), likely because both contain periods of Strombolian activity, lava effusion, and paroxysmal eruptions. However, plotting the frequency distributions of the two datasets (Fig. 4b) shows apparent differences that can be confirmed with simple statistical analysis. MIROVA night-time data between 2000 and 2014 have values between 0.001 MW and 2509 MW, and an arithmetic mean of 37.94 MW (variance 1.85×10^{16}), while values between 2015 and 2018 fall between 0.0008 MW and 6974 MW and have an arithmetic mean of 77.61 MW (variance 9.79×10^{16}). Applying a two-sided *t*-test to the populations indicates the difference in population statistics, with a t-statistic value of 4.58 and a p-value of 5.02×10^{-6}. Using the standard threshold of significance (α-value of 0.05), we can reject the null hypothesis that the 2000–2014 and 2015–2018 datasets are of the same distribution, and therefore state that night-time MIROVA values reveal a new eruptive regime beginning at Fuego in January 2015.

3.3. Correlating MIROVA with other data streams

Lyons et al. (2010) combined ground observations with radiative power values and lava flow lengths determined from MODIS observations to reveal a repeating pattern of passive lava effusion, followed by paroxysm then degassing explosions, at Fuego between 2005 and 2007. We use similar methods to present evidence that a new pattern of eruptive activity at Fuego began in January 2015, characterized by an increase in paroxysmal eruptions (both in frequency and in total energy), observable by changes in radiative power values. In order to study the new eruptive regime in greater detail, analysis was performed on a more comprehensive MIROVA dataset of Fuego from 2015 to 2018 that includes VRP values obtained from daytime MODIS data. A threshold of 200 MW[2] has been chosen to investigate the largest eruptions as this threshold (1) yields 166 above-threshold VRP values, and therefore provides a reasonably small dataset to study in detail; and (2) is extremely well-correlated with visual observations of above-background activity as recorded by special bulletins created and disseminated by INSIVUMEH. These bulletins document any occurrences of above-background activity of Fuego, and contain details of eruptive behaviour derived primarily from visual observations from OVFGO1 (for location, see Fig. 1). This documentation includes specific reporting of paroxysmal onset between 2015 and 2018. For this paper, paroxysm onset time is defined as the local time recorded by the INSIVUMEH special bulletin that first reports a paroxysm. INSIVUMEH determines paroxysmal onset by a number of parameters, including a steep relative increase in RSAM and observations of above-background activity (e.g. elevated number of summit explosions per hour, energetic lava fountaining) reported from OVFGO1 and OVFGO2. Several other monitoring parameters, including Washington VAAC reports and daily RSAM values derived from INSIVUMEH's seismometer on Fuego (FG3), also correspond to periods of above-background activity in 2015–2018. The significance of correlation between these datasets is discussed in Section 5.

[2] A magmatic source (1000 °C) with diameter 42 m is required to produce a VRP of 200 MW.

4. Results: changes in activity since 2015

4.1. Satellite observations of 21st-century (2000–2018) and recent (2015–2018) activity

A time-series of MIROVA[3] night-time data of Volcán de Fuego between January 2000 and June 2018 traces the activity of the volcano throughout the 21st century (Fig. 5). Several features are notable: the occurrence of occasional high-magnitude VRP values (≥1000 MW) between 2002 and 2007, on the order of 1–2 per year; the disappearance of such values between 2008 and early 2012; and the appearance, from early 2015, of ≥1000 MW values at considerably greater frequency than those appearing in 2002–2007 (all Fig. 5). These large-magnitude VRP values represent a series of closely-spaced, short-lived periods of high thermal radiation. VRP values for Fuego are not temporally consistent, but cumulative radiative energy (CRE) values for the entire period 2000–2018 can be derived by resampling VRP values to daily and weekly means, multiplying by daily or weekly time, and plotting the resulting cumulative values (Fig. 5b). A total CRE value of 1.70×10^{16} J (from daily mean) or 1.91×10^{16} J (from weekly mean) is found for Fuego from 2000 to 2018. Remarkably, almost half of this value is generated in the period 2015–2018 (7.25×10^{15} J for daily mean, 8.32×10^{15} J for weekly mean; see Fig. 5b).

A comparison of VRP values between (1) 2000–2018 and (2) 2015–2018 illustrates in further detail the increase both in frequency and in relative amplitude of large-magnitude VRP values beginning in January 2015 (Fig. 6). Although large-magnitude VRP values occur prior to 2015, they occur less frequently (217 values ≥ 1000 MW between 2000 and 2014 compared to 169 between 2015 and 2018). The largest VRP value to occur before 2015 is 2508 MW, on 16th March 2007; after 2015 is 6974 MW, occurring on 29th July 2016. Both of these values are associated with paroxysmal eruptions of Fuego and recorded by INSIVUMEH, as discussed later in this paper (see Section 4.2). The highest-magnitude peaks observed post-2015 do not always coincide with the largest paroxysmal eruption: the eruptions of 3rd June 2018 and 5th May 2017 are considered to be two of the largest since 1999, yet they are accompanied by relatively small thermal peaks.

A guiding study by Coppola et al. (2012) performed on MIROVA data from Stromboli between 2000 and 2011 stated that >90% of values in their dataset are <1 MW and can be excluded from analysis, as they are associated with overpasses taken during cloudy conditions, or at high angles. Although cloud cover is common at Fuego, MIROVA values from 2000 to 2018 are of noticeably greater value than from Stromboli: 3975 of 4412 (90.1%) VRP values are >1 MW, and 386 values (8.75%) are >100 MW, highlighting the remarkable radiative energy that Fuego has been emitting in recent years.

4.2. Correlating MIROVA observations with other data streams

The most informative and consistent data stream available against which to compare MIROVA values is the archive of special bulletins produced by INSIVUMEH during elevated activity. In the case of Volcán de Fuego, special bulletins are generated to report on the progress of a paroxysmal eruption, of lava effusion, or on descent of pyroclastic flows or of lahars. The correlation between large-magnitude VRP values and INSIVUMEH bulletins that report on paroxysmal eruptions is extremely strong (Fig. 7). According to INSIVUMEH, 12 paroxysms occurred in 2015, 15 in 2016, 12 in 2017, and two in the first half of 2018 (Global Volcanism Program, 2018; Table 1, this paper). Of the 166 occurrences of VRP values >200 MW between January 2015 and June 2018, 141 (84.9%) correlate to a paroxysmal eruption, where a VRP value is considered to be correlated to a paroxysm if it occurs within ±48 h of its onset. Of these 141 VRP values, 106 (75.1%) occurred at 0–48 h after paroxysm onset. Choosing 200 MW as a threshold means that there are no paroxysmal eruptions not accompanied by an above-threshold VRP value (i.e. no false negatives). However, 13 anomalies appear, i.e. above-threshold VRP values not associated with a paroxysmal eruption. These 13 anomalies occur in five clusters of time representing four distinct eruptive events: in 2015 (11th May; 27th September) and 2018 (16th April; 12th May; 21st May). A manual study of the MODIS images associated with these values shows they are real volcanogenic thermal anomalies i.e. they represent periods of elevated thermal activity at Fuego's summit. INSIVUMEH reported high activity including ash-rich explosions between 21st–26th May 2015, and again between 30th September and 1st October 2015, accompanied by incandescent fountaining, and avalanches and lava flows in Barrancas Santa Teresa and Trinidad. Nevertheless, a paroxysm did not follow. INSIVUMEH reported increased activity at Volcán de Fuego on 16th April 2018, with increased explosive activity and effusion of a 1300 m lava flow in Barranca Santa Teresa, although this was not followed by a paroxysmal eruption. The thermal anomalies of 12th and 21st May 2018 are connected in the same period of above-background activity. Fuego was moderately active on 12th May, generating frequent ash-rich explosions and incandescent fountaining from its summit. Lava effusion towards Barranca Ceniza began on 14th May, continuing until at least 21st May, when the flow had reached a length of 700–800 m. On this occasion the lava flow was not a precursor to paroxysmal eruption, as activity decreased and the flow stopped by 26th May.

Table 1 describes all paroxysmal eruptions between January 2015 and June 2018 and gives maximum VRP values associated with them, as well as occurrences of particular eruptive activity phenomena. An expanded version of Table 1, including a full description of eruptive activity contained in INSIVUMEH special bulletins, can be found in Appendix B.

From Table 1, we can recognize certain features that are typically associated with a paroxysmal eruption of Fuego between 2015 and 2018. In the days before a paroxysmal eruption, explosive activity at the summit increases in frequency and intensity, and audible degassing noises reminiscent of a steam locomotive can be heard (Lyons et al., 2010; Ruiz and Manzanillas, 2011). Eruptive behaviour evolves with more frequent audible degassing and more frequent and ash-rich summit explosions. The majority of paroxysmal eruptions (28 of 41, 68.2%) were reported to produce an incandescent fountain of several hundred metres above the summit crater. 40 of 41 (97.6%) paroxysms were accompanied by the effusion of lava flows in one or several of Fuego's barrancas. Of the bulletins that report both lava flows and incandescent lava fountaining, the majority state explicitly that lava flows are fed by the lava fountaining. All special bulletins reporting the onset of a paroxysmal eruption of Fuego explicitly state the estimated length of discharged lava flows, thus showing that lava flow effusion is a consistent precursor to paroxysmal eruption between January 2015 and June 2018. Lava flows associated with a paroxysm may achieve up to 3000 m in length. There does not appear to be a simple correlation between maximum lava flow length and maximum VRP value in paroxysms during this time. However, it should be noted that paroxysms at Fuego frequently produce several simultaneous lava flows in different barrancas, which is not illustrated by the Max lava length column (which records only the single longest lava flow of a paroxysm) so the lack of relationship between Max VRP value and Max lava length may be superficial only.

The appearance of short-lived, high-energy thermal peaks in the MIROVA night-time database of 2015–2018 can clearly be found in various other datasets that trace eruptive activity at Volcán de Fuego. For instance, frequent peaks in RSAM correlate closely with paroxysmal eruptions (Fig. 8b). Indeed, RSAM is a primary monitoring method for INSIVUMEH to assess the possibility of imminent paroxysmal activity at Fuego. The number of VAA reports generated monthly by the Washington Volcanic Ash Advisory Centre (VAAC) increases noticeably

[3] To the authors' knowledge, there have been no changes between 2000 and 2018 in the MODIS sensors that provide the data for MIROVA.

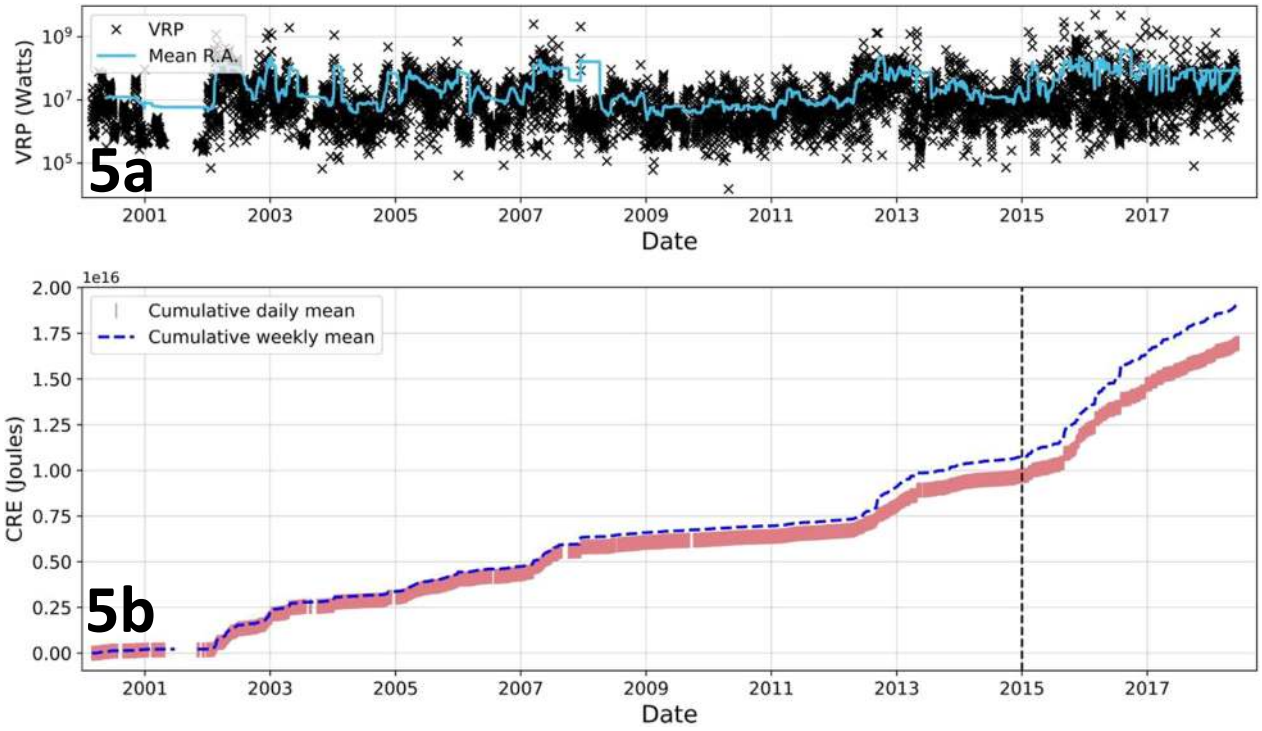

Fig. 5. a (above): Night-time VRP values from MIROVA track changes in activity at Volcán de Fuego throughout the period 2000–2018 (black crosses). A mean running average is illustrated by a solid blue line (annotated as 'Mean R.A.', panel a). Taking daily and weekly averages of VRP values allows for calculation of CRE emitted by Fuego throughout the period, as seen in panel b (below). Almost half of total CRE generated by Fuego in the period 2000–2018 was generated after 2015, as illustrated by dashed vertical line.
Data sourced from www.mirovaweb.it.

after January 2015 (Fig. 9). Fig. 9 shows the number of VAAs generated per month since the reawakening of Fuego in 1999. Of a total of 1932 VAAs generated between January 1999 and June 2018, over half (1352, 70.0%) were released between January 2015 and June 2018. A noticeable increase can be seen in the early period; for instance, the number of average monthly number of reports in 2014 was 7.5, compared to 13.7 in 2015 or 22.3 in 2016. However, it should be noted that this increase is unlikely to be due solely to increase in Fuego's activity. The Washington VAAC issue forecasts based on information from INSIVUMEH and pilots (among others), satellite data (including the GOES platform), and dispersion models. Factors causing the rise in monthly VAAC reports from Fuego since 2015 could include increased

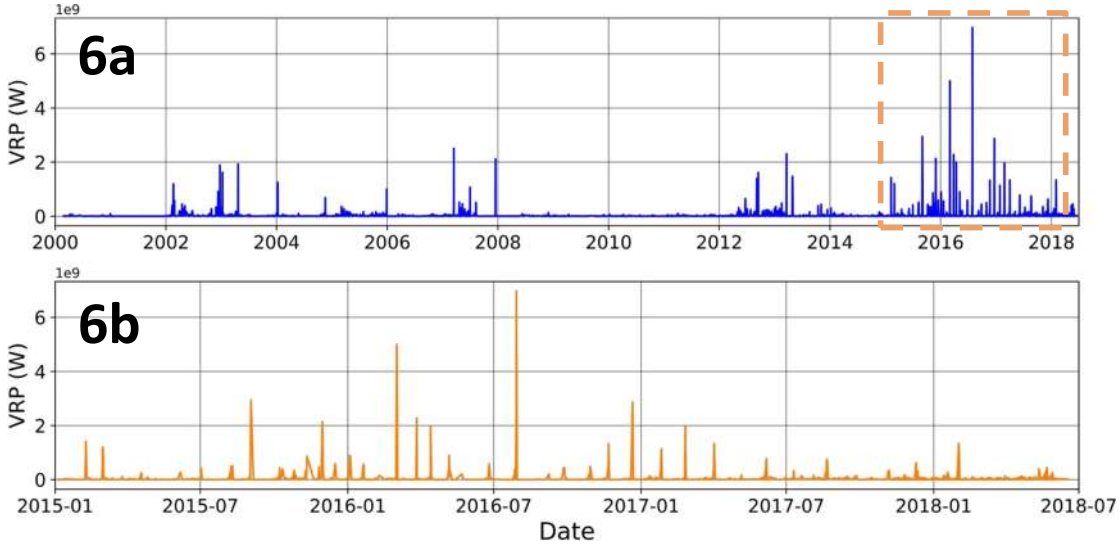

Fig. 6. a (above): Night-time VRP values from MIROVA track changes in activity at Volcán de Fuego throughout the period 2000–2018. Occasional peaks coincide with paroxysmal eruptions as recorded by INSIVUMEH (see Chapter 2). b (below): Marked increase in the frequency of large-magnitude VRP values occurs in 2015, with appearance of first short-lived thermal radiation peak on January 5th, 2015.

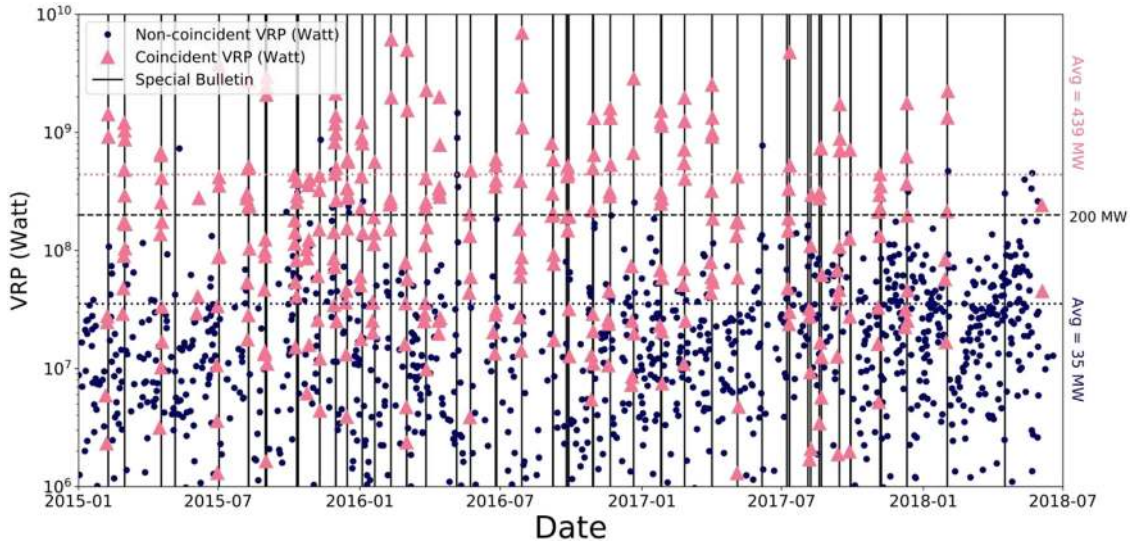

Fig. 7. Plot of all night-time VRP values from MIROVA and INSIVUMEH special bulletins between January 2015 and June 2018. Pink triangles represent VRP values coincident (±48 h) with INSIVUMEH bulletins (black vertical lines), while blue dots represent VRP values that occur >48 h before/after a special bulletin. Dashed black line represents threshold of 200 MW, above which all paroxysmal eruptions are associated with at least one VRP value. Dotted pink and blue lines represent average of all coincident and non-coincident MIROVA values (439.47 MW and 35.37 MW, respectively).

Table 1
Table of all paroxysms at Fuego, January 2015 to June 2018. Max VRP gives maximum VRP value associated with paroxysm (±48 h). Bulletin no. gives specific INSIVUMEH special bulletin in that year related to paroxysm (e.g. 004 for 2016 refers to bulletin #004-2016). Lava, Inc, A, PF, Lm refer to eruptive phenomena reported in special bulletins (respectively: lava, incandescent fountaining, avalanche, pyroclastic flow, and degassing sounds "like a locomotive train"). LL and EC refer to maximum lava flow length and eruptive column height (asl) recorded in any special bulletin associated with that paroxysm. Note that paroxysm may produce several lava flows; values stated here are only of single longest flow. For full table including details of all VRP values >200 MW Jan 2015–Jun 2018 (n = 166), see Appendix B.

Year	Date	No.	Max VRP (MW)	Bulletin no.	Lava	Inc	A	PF	Lm	LL (m)	EC (m)
2015	07/02/2015	1	1423.30	008, 015	X			X		1000	4300
	01/03/2015	2	1206.00	025	X	X				1600	5000
	18/04/2015	3	410.38	025	X	X				600	4800
	05/06/2015	4	277.92	033	X	X				1200	5000
	01/07/2015	5	3756.63	054, 055	X			X		1500	4500
	09/08/2015	6	2728.50	058, 059	X	X	X			3000	4700
	01/09/2015	7	2444.30	065, 070	X	X			X	800	5000
	10/10/2015	8	386.73	082	X	X			X	1200	4600
	26/10/2015	9	357.01	087	X			X	X	1500	4700
	09/11/2015	10	429.15	091	X	X			X	1800	5000
	30/11/2015	11	2132.39	101	X	X		X	X	3000	6000
	15/12/2015	12	338.57	105	X					800	4700
2016	03/01/2016	13	1220.44	004	X				X	3000	7300
	19/01/2016	14	563.63	008, 009	X	X		X	X	3000	6500
	10/02/2016	15	6126.95	024, 026	X	X	X	X	X	2000	5000
	01/03/2016	16	4998.34	031, 034	X		X			700	6000
	26/03/2016	17	2277.54	045	X				X	2000	6000
	13/04/2016	18	1993.77		X					2000	4800
	06/05/2016	19	1460.81		X	X	X		X	3000	5500
	22/05/2016	20	476.61	097, 099	X				X	1500	5000
	24/06/2016	21	347.75	114	X	X	X		X	2000	4800
	28/07/2016	22	2442.92	138	X	X	X	X	X	3000	5500
	07/09/2016	23	587.13	169, 171	X	X	X		X	1800	4900
	27/09/2016	24	517.99	180, 182	X	X	X		X	3500	4800
	29/10/2016	25	4279.08	189	X	X	X		X	1300	7000
	20/11/2016	26	1597.19	201	X	X	X		X	2500	5000
	20/12/2016	27	2866.18	210, 212	X	X	X	X	X	2000	5000
2017	26/01/2017	28	1222.48	004, 009	X	X	X	X	X	900	4800
	25/02/2017	29	1962.73	020	X	X	X			1600	5000
	01/04/2017	30	2531.27	034	X					2000	4800
	05/05/2017	31	423.56	046	X	X		X	X	2000	6000
	06/06/2017	32	774.13	068	X	X	X	X		500	6000
	11/07/2017	33	4782.65	096, 097	X	X				2300	5000
	07/08/2017	34	295.31	105	X	X	X			1300	4900
	21/08/2017	35	742.79	127	X				X	1400	5500
	13/09/2017	36	1733.03	148	X	X	X		X	500	4500
	28/09/2017	37	713.82	154, 157	X	X				600	4800
	05/11/2017	38	443.22	166, 170	X		X		X	1200	4800
	10/12/2017	39	1766.86	182, 187	X	X	X		X	1500	5000
2018	31/01/2018	40	1334.75	005, 011	X	X	X	X	X	800	4800
	03/06/2018	41	242.17	027, 028			x	X	X		10,000

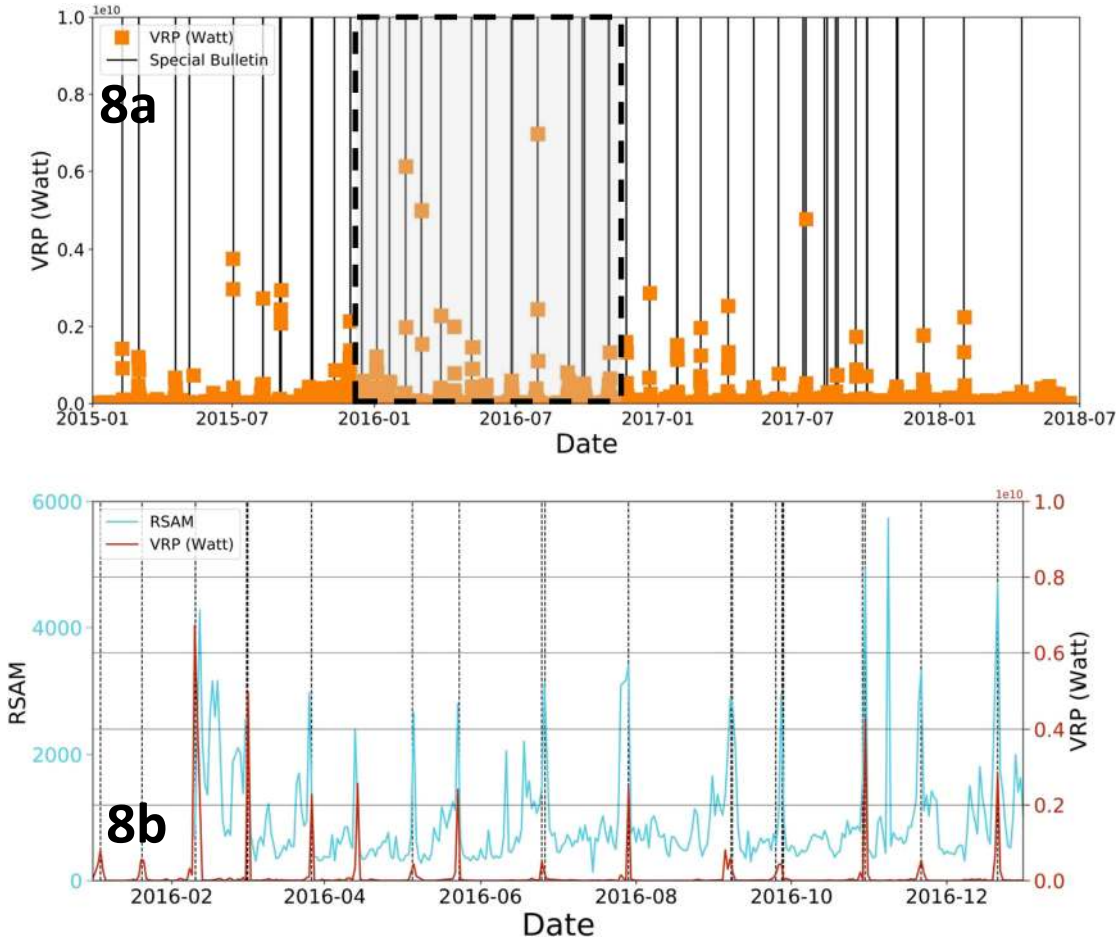

Fig. 8. a: (Above) Plot of MIROVA values January 2015–June 2018; y-axis is between 10^6 and 10^{10} W, to filter out low values associated with high angles or adverse viewing conditions. Vertical black lines show timings of all paroxysmal eruptions between 2015 and 2018 identified by INSIVUMEH through special bulletins. b: (Below) a subset of above plot, showing time-series of daily RSAM values (blue) against VRP values (red) derived from FG3 measurements. Timings of paroxysmal eruptions reported in INSIVUMEH special bulletins are plotted as dashed lines.

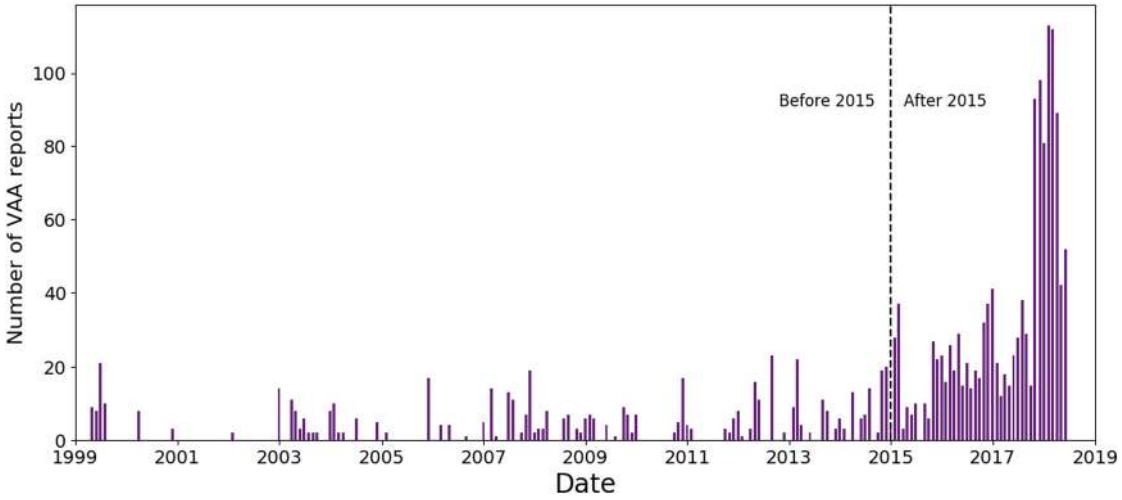

Fig. 9. Evidence for new cycle of activity illustrated by number of monthy ash advisory reports generated by Washington VAAC between January 1999 and June 2018. Dashed line indicates boundary between period of moderate activity 1999–2014 and period of elevated activity beginning January 2015.

reporting from INSIVUMEH and/or pilots to the VAAC, and more frequent imagery available since the launch of GOES-16 in November 2016.

5. Discussion

5.1. Paroxysmal eruptions following lava effusion at analogue volcanoes

There are few examples of paroxysmal eruptions consistently following lava effusion at other basaltic volcanoes. However, eruptions of Llaima volcano in Chile during an eruptive cycle that lasted between 2007 and 2009 show similar behaviour to post-2014 eruptions at Fuego (Romero Moyano et al., 2014). Eruptions of Etna in 1995–1996 (Allard et al., 2006) and 2011–2012 (Viccaro et al., 2015; Calvari et al., 2018; Giacomoni et al., 2018) also bear some comparison to Fuego's recent activity. In the days before a paroxysmal eruption, the increase of summit explosive activity produces a satellite-detectable increase of thermal anomalies at Fuego's summit (in terms of both intensity and frequency). Similar increases are also observed before Etna's paroxysms as documented in D'Aleo et al., 2018 (under review).

Sustained lava effusion preceding explosive paroxysm has been observed on multiple occasions at Stromboli (Polacci et al., 2009; Allard, 2010; Calvari et al., 2011). In particular, Stromboli's eruptions in 2002–2003 and 2007 involved slow lava effusion before paroxysm, inspiring several models that may have application to Fuego; indeed, some authors cite the similarity between the two systems (Calvari et al., 2011). Allard (2010) uses the collapsing foam model to explain the 2002–2003 and 2007 Strombolian paroxysms. Meanwhile, Calvari et al. (2011) interpret lava effusion during these periods as gradual decompression of Stromboli's magmatic system. The similar volume of lava erupted before each paroxysm (~0.004 km^3) suggests that the trigger for paroxysm is the eruption of a critical volume of material. Gradual lava effusion acts to increase the depth of the bubble-rich magma column in the conduit, drawing up less-porphyritic, volatile-rich magma from a deeper storage zone into the upper system, where it rises through the conduit and erupts explosively (i.e. the paroxysm). This model relies on several points of stability: of subsurface geometry, magma supply rate, and magma composition. A future avenue of exploration could be application of the Calvari et al. (2011) model to Fuego, by comparison of cumulative lava effusion volumes before individual paroxysmal eruptions.

Ripepe et al. (2017) focus on the same Strombolian paroxysms, with different conclusions. Persistent explosive activity does not fully clear the upper conduit, in which magma is stored and recycled. During pre-paroxysmal lava effusion, Ripepe et al. (2017) cite the increased contribution of a deep, volatile-rich magma that hampers magma recycling in the upper conduit; as lava effusion encourages the lower gas-rich source to rise through the conduit, the deep reservoir experiences fast decompression and further fuels the upper system with magma, eventually leading to paroxysm. This model changes the trigger of paroxysm from a perturbation at depth to changes in magmastatic conditions affecting decompression rate within the shallow subsurface. Invoking discharge from a shallow reservoir could explain the exceptional frequency of paroxysms seen at Fuego since 2015.

As complementary basaltic arc volcanoes, and for producing explosive paroxysms after sustained periods of lava flow effusion, there is merit in considering Stromboli, Etna, and Llaima as analogues with which to aid analysis of Fuego's behaviour. However, the paroxysmal eruptions that have occurred at Fuego since 2015 are extraordinary for both their consistency and their frequency. Furthermore, the crystal-poor magma produced by the Strombolian eruptions of 2002–2003 and 2007 is dissimilar to the strikingly crystal-rich of Fuego magmas (up to 40–50% phenocrysts in bombs erupted in 2017–18 pyroclastic flows (Hannah Moore, pers. comm.)). Nevertheless, there may be merit in applying the methods that produced the above models to Fuego's system. The installation of several broadband seismometers and an infrasound array at Fuego since the 3rd June 2018 eruption means that application of such methods is now possible.

5.2. Models for triggering paroxysms at Fuego

Lyons et al. (2010) propose two alternative models to explain a series of five paroxysmal eruptions observed at Fuego between 2005 and 2007. The first is the collapsing foam model introduced by Jaupart and Vergniolle (1988), where both effusive and explosive behaviours are caused by the accumulation, and subsequent release, of gas in an unstable foam layer. This hypothesis argues that lava effusion at surface is permitted by the accumulation of gas within a foam layer at a structural discontinuity in the magmatic subsurface. The eventual collapse of the foam layer into a gas slug that rises up the conduit drives Strombolian explosions and lava fountaining before the slug's arrival at surface. Such a model may produce similar behaviours to Fuego's if the viscosity or gas flux is high enough. The alternate hypothesis Lyons et al. (2010) propose for the trigger of Fuego's paroxysmal eruptions is the rise-speed dependent model advanced by Parfitt and Wilson (1995). This model differentiates between low magma rise speeds, where bubbles coalesce into slugs and rise to produce classic Strombolian activity, with higher speeds, where the smaller differential between bubbles and their carrying body impedes bubble coalescence. The ascending magma-gas mixture thus achieves the fragmentation threshold necessary to produce runaway coalescence much deeper in the conduit. An increase in magma rise speed, therefore, would be the driving force behind the transition from effusive to explosive eruptive activity seen at Fuego. However, Lyons et al. (2010) observed an increase in paroxysmal frequency during 2007, that coupled with a decrease in lava output disagree with the implications of the rise-speed dependent model, where higher effusion rates should correlate with more paroxysmal eruptions. Both parameters have increased at Fuego since 2015.

As with observations from 2005 to 2007, Fuego's activity since 2015 has consistently included lava effusion prior to paroxysm. Detection of VRP values >200 MW clearly indicates the presence of hot magma at the surface, which may anticipate a period of sustained lava effusion, elevated explosive activity at the summit, or both. However, lava effusion does not guarantee that a paroxysm is imminent. Episodes of elevated activity in 27th September 2015, 16th April and 12th–21st May 2018 generated lava flows but did not accelerate towards paroxysm. Compared to episodes of lava effusion that did culminate in paroxysm, these episodes are notable in producing lava flows of relatively minor length. Furthermore, effusion rates during these periods were relatively low: in May 2018, the lava flow grew 500 m in 48 h (12th–14th May), but effusion slowed with time, reaching 600 m on 18th May, and 700–800 m on 21st May. In comparison, episodes of lava flows culminating in paroxysm typically grow several kilometres in length within 48 h of first appearance; for example, the paroxysm of 28th–30th July 2016, where between 06:00 local time on 28th July and 14:30 on 29th July lava flows in Barrancas Santa Teresa and Las Lajas grew from 500 m and 1000 m to 3000 m each (see Appendix B for further information). This represents a significant increase in output from the paroxysms observed between 2005 and 2007, where similar flow lengths were achieved across months. It is also illustrated by the increase in cumulative energy seen in Fig. 3b. A possible explanation for this increase could be a rise of the magmatic column within Fuego's conduit, beginning in 2015 and maintained until 2018. This hypothesis has been proposed by Coppola et al. (2012) to explain the patterns in summit activity and effusive eruptions observed at Stromboli between 2000 and 2011.

What triggers a paroxysm at Volcán de Fuego? Petrographic analysis of eruptive products has provided the primary source of data to inform conceptual models of magma transport and evolution that may drive paroxysmal eruptions. The earliest of these models presented a system fed by a discrete pair of magma chambers: a small, dike-like chamber at several kilometres' depth, and a deeper chamber of greater volume (Rose et al., 1978; Martin and Rose, 1981). Later papers also cited the

possibility of a third, larger chamber near the crust-mantle boundary (Chesner and Rose, 1984). More recent literature invokes magma mixing across a range of depths rather than at discrete intervals (Roggensack, 2001; Berlo et al., 2012), with melt inclusions used to illustrate that material ejected in 1974 was sampled from a large range of depths prior to eruption (3–13 km) (Roggensack, 2001). Berlo et al. (2012) used melt inclusions to investigate the link between different eruptive episodes at Fuego and concluded that the eruptive episodes of 1974 and 1999 onwards were driven by episodic injections of magma from a deeper source to the shallow subsurface, followed by the ascent of magma parcels to the surface. Deposits from 2017 pyroclastic flows subject to petrographic analysis include heterogeneous crystal textures similar to those observed in samples studied by Berlo et al. (2012), suggesting a common inception (Hannah Moore, pers. comm.). The model by Berlo et al. (2012) that conceives of Fuego's paroxysms being fed by pulses of magma would discourage comparison with the Stromboli model offered by Calvari et al. (2011), which assumes a steady magmatic supply rate. An alternative explanation that has not previously been considered for triggering paroxysm at Fuego is the gravity-driven shedding of material from an ephemeral summit cone. In this model, persistent lava fountaining accumulates ballistic material in the summit crater as an ephemeral cone. Lava flow effusion begins when the full summit crater overspills. When travelling on a high initial slope angle, flows may pass the glass transition and deteriorate to fractured avalanches, before reagglutinating at lower altitudes as the slope angle decreases (Sumner, 1998; Escobar-Wolf, 2013). If the flow output rate were sufficiently high, lava flow effusion could destroy the ephemeral cone and remove enough volume to depressurize the magmatic system, thus triggering a paroxysmal eruption. In several paroxysms since 2015 Fuego had a visible depression in its the summit crater (e.g. 3rd January 2016): therefore, this model cannot work as a general explanation for triggering paroxysm. However, it may be invoked in specific cases where an ephemeral cone was observed prior to paroxysm (e.g. the paroxysms of 25th February 2017 and 12th October 2018).

There are several factors to consider regarding the methods used to study the accelerating cycle of explosive paroxysms observed at Fuego since 2015. Several of the largest paroxysms of this period (for example: 5th May 2017, 3rd June 2018) were associated with relatively small VRP values. Both paroxysms generated eruptive columns >6000 m asl and extensive pyroclastic flows, and the 5th May 2017 paroxysm produced extensive lava flows, yet neither was associated with a VRP value of >500 MW. A possible explanation may be attenuation of thermal anomalies tracked by MIROVA. The presence of meteorological clouds or volcanic plumes may cause partial or complete attenuation, as may the azimuth and zenith of the acquiring satellite relative to the source of thermal anomaly. These factors are difficult to quantify and must be evaluated on an image-by-image basis. Some of the bias caused by these factors may be removed by introducing a minimum threshold below which VRP values may be excluded, assuming they represent values taken under cloudy conditions or at extreme acquisition geometries (Coppola et al., 2012). An alternative interpretation could be that these paroxysms did not generate large VRP values because the majority of the eruptive volume they produced was in the form of pyroclastic flow material. In this case, the fine-grained material composing much of these flows cools rapidly (within hours), and would not produce a strong radiative power signal detectable by MIROVA. If this were true, the resulting bias would unfortunately not be mitigated by introduction of a minimum inclusion threshold. Ultimately, the absolute value of any single VRP measurement may be affected by any of the factors mentioned above, and direct comparison between individual VRP values may be biased. Nevertheless, there remains strong evidence for the association between VRP values >200 MW and thermal emission from hot surfaces including lava flows, incandescent fountaining, and Strombolian eruptions that represent above-background activity (including paroxysmal eruption) at Fuego.

5.3. Implications for eruptive hazards

Although the flanks of Volcán de Fuego were populated when the 1974 eruptive episode occurred, academic literature contains few references to the impacts of the episode on these populations. Nevertheless, the tephra and pyroclastic flow material generated likely had impacts similar to those caused by the large-magnitude eruptions in 1971 and 1973, elaborated on by Bonis and Salazar (1973). In the 44 years since the 1974 eruption, the lands that surround Fuego have undergone considerable development. There are schools, residential communities, and industrial facilities near the volcano. RN-14, the highway that serves as the principal trade route between Mexico and Guatemala, crosses several rivers which drain the Fuego volcanic area and are primary lahar routes (see Fig. 1). Many tens of thousands of people live near Fuego: >50,000 live within 10 km, and >1,000,000 within 30 km, of its summit (GVP, 2018). The majority of these people live in poverty, relying on agriculture for their livelihood (Graves, 2007; INE, 2013). The various hazards associated with Fuego have previously been considered, both in USGS reports and in hazard maps produced by INSIVUMEH following the 3rd June 2018 eruption (Vallance et al., 2001; INSIVUMEH, 2018). We focus below on the implications of this study's results for the understanding of these hazards.

The most severe and immediate hazard of Volcán de Fuego, in the case of a large-magnitude explosive paroxysm, is pyroclastic flows; and the regions most obviously vulnerable to pyroclastic flow hazard are those located close to Fuego's barrancas. Communities such as Sangre de Cristo (located at OVFGO2 in Fig. 1) have been evacuated multiple times since 2015 because of risk deriving from paroxysm-generated pyroclastic flows. More recently and devastatingly, pyroclastic flows generated by the 3rd June 2018 eruption travelled >12 km down Barranca Las Lajas and destroyed both the Las Lajas bridge and the community of San Miguel Los Lotes, killing several hundred people (for locations, see Fig. 1). Preliminary estimates put the pyroclastic flow deposit volume in Barranca Las Lajas somewhere between 20 and 30 million m^3. This figure is comparable to volume estimates for pyroclastic flows produced by explosive paroxysms between 1999 and 2018: for instance, the 21st May 1999 eruption produced 0.0255 km^3 of pyroclastic flow material, and the 13th September 2012 eruption produced 0.0269 km^3 (Escobar-Wolf, 2013). However, the greater frequency of paroxysms and paroxysm-generated pyroclastic flows since 2015 has important hazard implications because of the more frequent exposure of nearby communities to risk deriving from those hazards. Furthermore, paroxysms occurring since 2015 illustrate two points regarding risk generated from pyroclastic flows of Fuego: first, that during a paroxysm, pyroclastic flows are typically generated in multiple barrancas, thus simultaneously increasing risk in multiple areas; second, that pyroclastic flows may be a major hazard to communities beyond those closest to barrancas. San Miguel Los Lotes was not considered to be especially at risk of pyroclastic flow, but the sequential descent of multiple flows down Barranca Las Lajas may have filled the barranca and caused overspill further down Fuego's flanks. The increase of paroxysms since 2015 has important pyroclastic flow hazard implications both at the moment of descent and subsequently, due to the greater accumulation of material.

Airborne ash and ash fall from eruptions of Volcán de Fuego have persistently affected both local and distant populations in Guatemala. Due to the hazard airborne ash presents to planes, air traffic corridor R644, which runs close to the volcano and was primarily used for traffic to Mexico, is now permanently closed, resulting in rerouting of flights (Ivan Velasquez, pers. comm.). This is a direct result of the increase in explosive paroxysms since 2015. Eruptions smaller than those of 1974 have produced tephra that has had significant impact; the eruption of 13th September 2012 forced the closure of La Aurora International Airport in Guatemala City for three days, costing the country millions of dollars in revenue. An increase in paroxysmal frequency could have similar or greater economic impact. Meanwhile, tephra fallout will be

the principal far-reaching hazard of a future paroxysm, potentially severely impacting Guatemala City (40 km E of Fuego), or Quetzaltenango (80 km NW), i.e. one of the two largest Guatemalan cities. Closer to Fuego, the negative impact of regular ash fall caused by frequent paroxysms on crop productivity is unstudied but potentially significant.

An intense annual rainy season in Guatemala, combined with the large volume of pyroclastic material deposited on Fuego's flanks, ensure that lahars from the volcano are frequent and powerful. Lahars may reach extraordinary dimensions of over 40 m width and 4 m depth and speeds >8 m/s (Schilling, 2001; Escobar-Wolf, 2013). Lahars generated since 2015 can be exceptionally long-ranging: in August 2017 they destroyed a Scout camp (known as "Finca Scout", located 14.34°N, 90.95°W; see FS on Fig. 1) and a bridge that borders the Ceniza river 20 km downstream of Fuego. The massive volume of pyroclastic material deposited since 2015 will supply future large lahars, with both direct hazards and resulting hazards associated with sediment transport in the rivers draining Fuego. Lahars from Fuego do not only occur during eruption, and associated risks are always present.

If the current magmatic conditions at Fuego persist, one would expect that the frequent paroxysmal eruptions seen in 2015–2018 would continue throughout 2018 and beyond. Indeed, paroxysmal eruptions occurring on 12th October and 18th November suggest this is the case. However, the eruption of June 3rd, 2018 was of a different character from other paroxysms in this period: preceded by a greater period of quiescence, and possibly not preceded by lava effusion.[4] Therefore, it is possible that the frequent paroxysms that have characterized Fuego's recent activity will not continue. Alternatively, the 3rd June eruption could herald another period of extraordinarily high activity, just as activity in the early 1970s included large eruptions in 1971 and 1973 and a cluster of sub-Plinian eruptive activity in 1974. Lyons et al. (2010) did note the increase in paroxysmal frequency during their period of observation (2005–2007) and suggest that the observed increase in explosive activity could suggest a transition to less open-vent conditions, with significant hazard implications. In that case the increase preceded a 5-year hiatus in paroxysms. Of course, past behaviour is not necessarily an indicator of future activity. However, the increase in paroxysmal frequency since 2015 re-emphasises this concern and underscores the need for continued study of Fuego's paroxysmal eruptions as a critical factor in future risk mitigation efforts.

6. Conclusions

Volcán de Fuego's frequent activity and geographical situation renders it an ideal subject for synchronous study of eruptive activity and volcanic hazard. The sub-Plinian eruptive episode of October 1974 has allowed analyses of the subsurface magmatic system of Fuego, while eruptions between 1971 and 1974 have highlighted the possibility of multiple large-magnitude eruptions occurring in sequential years at Fuego.

A new eruptive regime beginning in January 2015 and characterized by regular paroxysmal eruptions consistently preceded by lava effusion can be traced in satellite remote sensing data and corroborated by seismic and visual observations. Tracing the details of the new eruptive regime allows for consideration of various models to explain the triggering cause for paroxysm. While further study is required to elucidate trigger(s) of paroxysm at Fuego, there may be merit in considering recent models based on behaviour of Stromboli, where paroxysm is triggered by decompression of the shallow conduit by lava effusion. We propose that the MIROVA database is an effective tool for comprehending long-term changes in eruptive activity at Volcán de Fuego, and may significantly improve volcano monitoring capacity at Fuego, and possibly at other open-vent systems.

[4] As mentioned in Section 5.2, the presence of meteorological cloud is a possible explanation for attenuation of VRP signal. Both ground-based observations and satellite detection agree on the presence of cloud throughout much of the 3rd June 2018 eruption.

The eruption of 3rd June 2018 killed hundreds of people in San Miguel Los Lotes and destroyed La Reunion resort, and tragically showed the potential of these paroxysmal eruptions to cause great damage. INSIVUMEH and CONRED are acting with the international volcanological community and local communities to prepare for another such paroxysm, by increasing hazard monitoring and forecasting for Fuego, and producing a series of hazard assessments. Mitigation of risks associated with persistent activity of Fuego will require continued cooperation between these groups.

Supplementary data to this article can be found online at https://doi.org/10.1016/j.jvolgeores.2019.01.001.

Author contributions

The project was conceived by IMW and AKN. REW provided data and contributed significantly both to the Discussion and general direction of the manuscript. HET contributed significantly to the Discussion. DC provided MIROVA data and contributed to analysis. GC and CCQ provided RSAM data and INSIVUMEH bulletins and contributed to discussion of timelines. All authors listed have made a substantial and intellectual contribution to the work and approved it for publication.

Statement of competing interests

The authors have no competing interests to declare.

Acknowledgements

This work was supported by the Natural Environment Research Council. We gratefully acknowledge the support of scientists and staff at INSIVUMEH in making this work possible. We give thanks to the two referees whose comments and guidance significantly informed and improved the paper, and we appreciate the constructive comments of an anonymous reviewer whose input greatly helped an earlier version of this manuscript. This work was partly funded by NERC grants NE/L002434/1 (AKN) and NE/P006744/1 (HET).

References

Allard, P., 2010. A CO_2-rich gas trigger of explosive paroxysms at Stromboli basaltic volcano, Italy. J. Volcanol. Geotherm. Res. 189 (3–4), 363–374. https://doi.org/10.1016/j.jvolgeores.2009.11.018.

Allard, P., Behncke, B., D'Amico, S., Neri, M., Gambino, S., 2006. Mount Etna 1993–2005: anatomy of an evolving eruptive cycle. Earth Sci. Rev. 78 (1–2), 85–114. https://doi.org/10.1016/j.earscirev.2006.04.002.

Álvarez-Gómez, J.A., Meijer, P.T., Martínez-Díaz, J.J., Capote, R., 2008. Constraints from finite element modelling on the active tectonics of northern Central America and the Middle America Trench. Tectonics 27 (1). https://doi.org/10.1029/2007TC002162.

Andres, R.J., Rose, W.I., Stoiber, R.E., Williams, S.N., Matías, O., Morales, R., 1993. A summary of sulphur dioxide emission rate measurements from Guatemalan volcanoes. Bull. Volcanol. 55 (5), 379–388. https://doi.org/10.1007/BF00301150.

Authemayou, C., Brocard, G., Teyssier, C., Simon-Labric, T., Gutiérrez, A., Chiquín, E.N., Morán, S., 2011. The Caribbean–North America–Cocos Triple Junction and the dynamics of the Polochic–Motagua fault systems: pull-up and zipper models. Tectonics 30 (3). https://doi.org/10.1029/2010TC002814.

Berlo, K., Stix, J., Roggensack, K., Ghaleb, B., 2012. A tale of two magmas, Fuego, Guatemala. Bull. Volcanol. 74 (2), 377–390. https://doi.org/10.1007/s00445-011-0530-8.

Bonis, S., Salazar, O., 1973. The 1971 and 1973 eruptions of Volcan Fuego, Guatemala, and some socio-economic considerations for the volcanologist. Bull. Volcanol. 37 (3), 394–400. https://doi.org/10.1007/BF02597636.

British Broadcasting Corporation (BBC), 2012. Guatemala Fuego volcano triggers evacuation. Retrieved from:. http://www.bbc.co.uk/news/world-latin-america-19594481, Accessed date: 12 July 2018.

Burkart, B., Self, S., 1985. Extension and rotation of crustal blocks in northern Central America and effect on the volcanic arc. Geology 13 (1), 22–26. https://doi.org/10.1130/0091-7613(1985)13<22:EAROCB>2.0.CO;2.

Calvari, S., Spampinato, L., Bonaccorso, A., Oppenheimer, C., Rivalta, E., Boschi, E., 2011. Lava effusion—a slow fuse for paroxysms at Stromboli volcano? Earth Planet. Sci. Lett. 301 (1–2), 317–323. https://doi.org/10.1016/j.epsl.2010.11.015.

Calvari, S., Cannavo, F., Bonaccorso, A., Spampinato, L., Pellegrino, A.G., 2018. Paroxysmal explosions, lava fountains and ash plumes at Etna volcano: eruptive processes and hazard implications. Front. Earth Sci. 6, 107. https://doi.org/10.3389/feart.2018.00107.

Chesner, C.A., Rose Jr., W.I., 1984. Geochemistry and evolution of the Fuego volcanic complex, Guatemala. J. Volcanol. Geotherm. Res. 21 (1–2), 25–44. https://doi.org/10.1016/0377-0273(84)90014-3.

de Ciudad-Real, A., 1873. Relacion breve y verdadera de algunas cosas de las muchas que sucedieron al Padre Fray Alonso Ponce en las provincias de la Nueva España, siendo comisario general de aquellas partes. Tomo I. Imprenta de la Viuda de Calero (Madrid).

Co-ordinadora Nacional para la Reducción de Desastres, CONRED, 2018. #VolcánDeFuego Te compartimos los datos de personas albergadas, atendidas e incidentes registrados hasta el momento por la erupción del volcán de Fuego. #PrevenirParaVivir #TodosSomosResponsables. 19 June 2018 Retrieved from:. https://twitter.com/ConredGuatemala/status/1009088485368745985, Accessed date: 12 April 2018.

Coppola, D., Piscopo, D., Laiolo, M., Cigolini, C., Delle Donne, D., Ripepe, M., 2012. Radiative heat power at Stromboli volcano during 2000–2011: twelve years of MODIS observations. J. Volcanol. Geotherm. Res. 215 (48–60). https://doi.org/10.1016/j.jvolgeores.2011.12.001.

Coppola, D., Laiolo, M., Cigolini, C., Delle Donne, D., Ripepe, M., 2016. Enhanced volcanic hot-spot detection using MODIS IR data: results from the MIROVA system. In: Harris, A.J.L., De Groeve, T., Garel, F., Carn, S.A. (Eds.), Detecting, Modelling and Responding to Effusive Eruptions. Geological Society, London, Special Publications 426(181–2015). https://doi.org/10.1144/SP426.5.

D'Aleo, R., Bitetto, M., Delle Donne, D., Coltelli, M., Coppola, D., McCormick Kilbride, B., Pecora, E., Ripepe, M., Salem, L., Tamburello, G., Aiuppa, A., 2018. Understanding the SO2 degassing budget of Mt Etna's paroxysms: first examples from the December 2015 sequence. Front. Earth Sci. https://doi.org/10.3389/feart.2018.00239 (provisionally accepted).

Davies, D.K., Quearry, M.W., Bonis, S.B., 1978. Glowing avalanches from the 1974 eruption of the volcano Fuego, Guatemala. Geol. Soc. Am. Bull. 89 (3), 369–384. https://doi.org/10.1130/0016-7606(1978)89<369:GAFTEO>2.0.CO;2.

Degger, E., 1932. Der Ausbruch des Vulkans "Fuego" in Guatemala amd 21 Januar 1932 und die chemische Zusammensetzung seiner Auswurfsmaterialien. Chem. Erde 7 (291–297).

Escobar-Wolf, R., 2013. Volcanic Processes and Human Exposure as Elements to Build a Risk Model for Volcan de Fuego, Guatemala. (PhD thesis). Retrieved from:. https://digitalcommons.mtu.edu/etds/638, Accessed date: 12 May 2018.

Feldman, L., 1993. Mountains of fire, lands that shake. Earthquakes and Volcanic Eruptions in the Historic Past of Central America (1505–1899). Labyrinthos, California.

Giacomoni, P.P., Coltorti, M., Mollo, S., Ferlito, C., Braiato, M., Scarlato, P., 2018. The 2011–2012 paroxysmal eruptions at Mt. Etna volcano: insights on the vertically zoned plumbing system. J. Volcanol. Geotherm. Res. 349 (370–391). https://doi.org/10.1016/j.jvolgeores.2017.11.023.

Global Volcanism Program (GVP), 2018. In: Venzke, E. (Ed.), [Fuego (342090)] in Volcanoes of the World, v. 4.6.7. Smithsonian Institution https://volcano.si.edu/volcano.cfm?vn=342090, Accessed date: 29 May 2018.

Google Earth V 7.1.8.3036, (22 March, 2018). Volcán de Fuego, Guatemala. 14° 28' 23.90"N, 90° 52' 53.34" W, eye alt 14.04 km. Digital Globe 2018 [28 July, 2018]. http://www.earth.google.com.

Graves, K., 2007. Risk Perception of Natural Hazards in the Volcanic Regions of Ecuador and Guatemala. (Master's thesis). Retrieved from:. https://www.mtu.edu/social-sciences/graduate/theses-dissertations/eep-theses/index.html, Accessed date: 12 July 2018.

Hutchison, A.A., Cashman, K.V., Williams, C.A., Rust, A.C., 2016. The 1717 eruption of Volcán de Fuego, Guatemala: cascading hazards and societal response. Quat. Int. 394 (69–78). https://doi.org/10.1016/j.quaint.2014.09.050.

Instituto Nacional de Estadística (INE), 2013. Caracterización Estadistica de Guatemala. Retrieved from:. http://www.ine.gob.gt/index.php/estadisticas/caracterizacion-estadistica, Accessed date: 12 July 2018.

Instituto Nacional de Sismología, Vulcanología, Meteorología e Hidrología (INSIVUMEH), 2012a. Folleto sobre Volcán de Fuego. Retrieved from:. http://www.insivumeh.gob.gt, Accessed date: 12 July 2018.

Instituto Nacional de Sismología, Vulcanología, Meteorología e Hidrología (INSIVUMEH), 2012b. Reporte preliminar de la erupción del Volcán de Fuego 13 de septiembre 2012. Retrieved from:. http://www.insivumeh.gob.gt/folletos/REPORTE%20ERUPCION%20DE%20FUEGO%2013%20SEP%202012%20%28OK%29.pdf, Accessed date: 12 July 2018.

Instituto Nacional de Sismología, Vulcanología, Meteorología e Hidrología (INSIVUMEH), 2018. Mapa de Amenaza Volcanica No.s 14, 15, 16 (Volcán Fuego Lahar Escenario A, Volcán Fuego Lahar Escenario B, Volcán de Fuego, Flujos Piroclásticos). Retrieved from:. http://www.insivumeh.gob.gt/?page_id=578, Accessed date: 12 July 2018.

Jaupart, C., Vergniolle, S., 1988. Laboratory models of Hawaiian and Strombolian eruptions. Nature 331 (6151), 58. https://doi.org/10.1038/331058a0.

Kurtz, A.W., 1913. Documentos Antiguos: Copia de dos cartas manuscritas de Don Pedro de Alvarado a Hernando Cortes, 11 de abril y 28 de julio 1524. Tip. – Arenales hijos. Retrieved from:. https://www.scribd.com/doc/213352772/Cartas-de-Pedro-de-Alvarado-a-Hernan-Cortes, Accessed date: 12 July 2018.

Lyons, J.J., Waite, G.P., 2011. Dynamics of explosive volcanism at Fuego volcano imaged with very long period seismicity. J. Geophys. Res. Solid Earth 116 (B9). https://doi.org/10.1029/2011JB008521.

Lyons, J.J., Johnson, J.B., Waite, G.P., Rose, W.I., 2007. Observations of cyclic Strombolian eruptive behavior at Fuego volcano, Guatemala reflected in the seismo-acoustic record. AGU Fall Meeting Abstracts Retrieved from:. http://adsabs.harvard.edu/abs/2007AGUFM.V11C0745L, Accessed date: 12 July 2018 (December).

Lyons, J.J., Waite, G.P., Rose, W.I., Chigna, G., 2010. Patterns in open vent, strombolian behavior at Fuego volcano, Guatemala, 2005–2007. Bull. Volcanol. 72 (1), 1. https://doi.org/10.1007/s00445-009-0305-7.

Martin, D.P., Rose Jr., W.I., 1981. Behavioral patterns of Fuego volcano, Guatemala. J. Volcanol. Geotherm. Res. 10 (1–3), 67–81. https://doi.org/10.1016/0377-0273(81)90055-X.

Nadeau, P.A., Palma, J.L., Waite, G.P., 2011. Linking volcanic tremor, degassing, and eruption dynamics via SO_2 imaging. Geophys. Res. Lett. 38 (1). https://doi.org/10.1029/2010GL045820.

National Oceanic and Atmospheric Administration (NOAA), 2019. Current Volcanic Ash Advisories: Washington VAAC. Retrieved from:. https://www.ssd.noaa.gov/VAAC/messages.html, Accessed date: 14 January 2018.

Pardini, F., Queißer, M., Naismith, A., Watson, I.M., Clarisse, L., Burton, M., 2019. Initial constraints on triggering mechanisms of the eruption of Fuego volcano (Guatemala) from 3 June 2018 using IASI satellite data. J. Volcanol. Geotherm. Res. (Submitted, Revision made 23 November 2018).

Parfitt, E.A., Wilson, L., 1995. Explosive volcanic eruptions—IX. The transition between Hawaiian-style lava fountaining and Strombolian explosive activity. Geophys. J. Int. 121 (1), 226–232 Retrieved from:. http://adsabs.harvard.edu/full/1994LPI....25.1049P, Accessed date: 12 July 2018.

Patrick, M.R., Harris, A.J., Ripepe, M., Dehn, J., Rothery, D.A., Calvari, S., 2007. Strombolian explosive styles and source condition: insights from thermal (FLIR) video. Bull. Volcanol. 69 (7), 769–784. https://doi.org/10.1007/s00445-006-0107-0.

Polacci, M., Baker, D.R., Mancini, L., Favretto, S., Hill, R.J., 2009. Vesiculation in magmas from Stromboli and implications for normal Strombolian activity and paroxysmal explosions in basaltic systems. J. Geophys. Res. Solid Earth 114 (B1). https://doi.org/10.1029/2008JB005672.

Rader, E., Geist, D., Geissman, J., Dufek, J., Harpp, K., 2015. Hot clasts and cold blasts: thermal heterogeneity in boiling-over pyroclastic density currents. Geol. Soc. Lond., Spec. Publ. 396 (1), 67–86. https://doi.org/10.1144/SP396.16.

Ripepe, M., Pistolesi, M., Coppola, D., Delle Donne, D., Genco, R., Lacanna, G., ... Valade, S., 2017. Forecasting effusive dynamics and decompression rates by magmastatic model at open-vent volcanoes. Sci. Rep. 7 (1), 3885. https://doi.org/10.1038/s41598-017-03833-3.

Roggensack, K., 2001. Unraveling the 1974 eruption of Fuego volcano (Guatemala) with small crystals and their young melt inclusions. Geology 29 (10), 911–914. https://doi.org/10.1130/0091-7613(2001)029<0911:UTEOFV>2.0.CO;2.

Romero Moyano, J., Keller Ulrich, W., Marfull, V., 2014. Short chronological analysis of the 2007–2009 eruptive cycle and its nested cones formation at Llaima volcano. J. Technol. Possibilism 2 (3), 1–9 Retrieved from. https://www.researchgate.net/profile/Jorge_Romero10/publication/259584302_Short_chronological_analysis_of_the_2007-2009_eruptive_cycle_and_its_nested_cones_formation_at_Llaima_volcano/links/0c96052ccb47d81873000000/Short-chronological-analysis-of-the-2007-2009-eruptive-cycle-and-its-nested-cones-formation-at-Llaima-volcano.pdf, Accessed date: 12 July 2018.

Rose Jr., W.I., Anderson Jr., A.T., Woodruff, L.G., Bonis, S.B., 1978. The October 1974 basaltic tephra from Fuego volcano: description and history of the magma body. J. Volcanol. Geotherm. Res. 4 (1–2), 3–53. https://doi.org/10.1016/0377-0273(78)90027-6.

Rose, W.I., Self, S., Murrow, P.J., Bonadonna, C., Durant, A.J., Ernst, G.G.J., 2008. Nature and significance of small volume fall deposits at composite volcanoes: Insights from the October 14, 1974 Fuego eruption, Guatemala. Bull. Volcanol. 70 (9), 1043–1067. https://doi.org/10.1007/s00445-007-0187-5.

Ruiz, M.C., Manzanillas, L., 2011. Analysis of chugging signals from Reventador volcano, Ecuador. AGU Fall Meeting Abstracts, 1-2591 Retrieved from:. http://adsabs.harvard.edu/abs/2011AGUFM.V53A2591R, Accessed date: 8 August 2018.

Schilling, S., 2001. Lahar Hazards of Fuego Volcano, Guatemala. US Geological Survey Retrieved from:. https://pubs.usgs.gov/of/2001/0431/pdf/of2001-0431_plate1.pdf, Accessed date: 12 July 2018.

Stoiber, R., Carr, M., 1973. Quaternary volcanic and tectonic segmentation of Central America. Bull. Volcanol. 37 (3), 304–325. https://doi.org/10.1007/BF02597631.

Sumner, J., 1998. Formation of clastogenic lava flows during fissure eruption and scoria cone collapse: the 1986 eruption of Izu-Oshima Volcano, eastern Japan. Bull. Volcanol. 60, 195. https://doi.org/10.1007/s004450050227.

Tedlock, D., 1985. Popol Vuh: The Definitive Edition of the Mayan Book of the Dawn of Life and the Glories of Gods and Kings. 2nd ed. Simon and Schuster, New York.

Vallance, J.W., Siebert, L., Rose Jr., W.I., Girón, J.R., Banks, N.G., 1995. Edifice collapse and related hazards in Guatemala. J. Volcanol. Geotherm. Res. 66 (1–4), 337–355. https://doi.org/10.1016/0377-0273(94)00076-S.

Vallance, J.W., Schilling, S.P., Matías, O., Rose, W., Howell, M.M., 2001. Volcano Hazards at Fuego and Acatenango, Guatemala. US Geological Survey Retrieved from:. https://pubs.usgs.gov/of/2001/0431/, Accessed date: 12 July 2018.

VanKirk, J., Bassett-VanKirk, P., 1996. Remarkable Remains of the Ancient Peoples of Guatemala. University of Oklahoma Press, Norman, Oklahoma.

Viccaro, M., Calcagno, R., Garozzo, I., Giuffrida, M., Nicotra, E., 2015. Continuous magma recharge at Mt. Etna during the 2011–2013 period controls the style of volcanic activity and compositions of erupted lavas. Mineral. Petrol. 109 (1), 67–83. https://doi.org/10.1007/s00710-014-0352-4.

Volcano Global Risk Identification & Analysis Project (VOGRIPA), 2018. . Retrieved from:. http://www.bgs.ac.uk/vogripa/index.cfm, Accessed date: 12 July 2018.

Waite, G.P., Nadeau, P.A., Lyons, J.J., 2013. Variability in eruption style and associated very long period events at Fuego volcano, Guatemala. J. Geophys. Res. Solid Earth 118 (4), 1526–1533. https://doi.org/10.1002/jgrb.50075.

Webley, P.W., Wooster, M.J., Strauch, W., Saballos, J.A., Dill, K., Stephenson, P., ... Matias, O., 2008. Experiences from near-real-time satellite-based volcano monitoring in Central America: case studies at Fuego, Guatemala. Int. J. Remote Sens. 29 (22), 6621–6646. https://doi.org/10.1080/01431160802168301.

Wooster, M.J., Zhukov, B., Oertel, D., 2003. Fire radiative energy for quantitative study of biomass burning: derivation from the BIRD experimental satellite and comparison to MODIS fire products. Remote Sens. Environ. 86 (1), 83–107. https://doi.org/10.1016/S0034-4257(03)00070-1.